New Vistas in Polymer Degradation. Thermal Oxidation Processes in Poly(ether imide)

Sabrina Carroccio*,† and Concetto Puglisi

Istituto di Chimica e Tecnologia dei Polimeri, Consiglio Nazionale delle Ricerche, Viale A. Doria, 6-95125 Catania, Italy

Giorgio Montaudo*,‡

Dipartimento di Scienze Chimiche, Università di Catania, Viale A. Doria, 6-95125 Catania, Italy

Received February 2, 2005; Revised Manuscript Received May 27, 2005

ABSTRACT: Poly{2,2-bis[4-(3,4-dicarboxyphenoxy)phenyl]propane dianhydride−1,3-phenylendiamine} copolymer (ULTEM) was subjected to thermoaging in an attempt to determine the structure of the species formed during oxidative degradation. The oxidative process was followed as a function of exposure time by using MALDI−TOF MS. Thermal oxidation produces charring after only 15 min and the formation of insoluble residue amounts to 50% after 180 min at 350°C. Highly valuable structural information (including the end groups) was extracted from the MALDI spectra of the thermally oxidized ULTEM soluble samples. Oxidized specimens contained acetophenone, phenylacetic acid, phenols, benzoic acid, bisphenol A, phthalimide, and phthalic anhydride end groups. The mechanisms accounting for their formation involve several reactions: (i) cleavage of the diphenyl ether units; (ii) oxidative degradation of the isopropylidene bridge of BPA units; (iii) thermal cleavage of phenylphthalimide units.

Introduction

In the past decade the structural analysis of polymers has taken advantage of the development of MALDI (matrix assisted laser desorption ionization−time-of-flight mass spectrometry), a highly sensitive, nonaveraging technique that allows the determination of individual species contained in a polymer sample.[1−3]

Studies on oxidation mechanisms are crucial for the understanding of aging processes in polymers. However, mechanisms reported in the literature are often inferred from the observation of relatively few end products.[4−7] Molecules formed by oxidation are often very reactive, do not accumulate, and are present only in minor amounts among the ultimate reaction products. Conventional techniques (IR spectroscopy for instance) may yield information on functional groups, but not on the structure and end groups of the whole molecule.

On the contrary, MALDI spectra yield precise information on the size, structure and end groups of oligomers originated in the oxidation process, allowing discrimination among possible oxidation pathways.[1,2]

Applications of MALDI to the study of polymer oxidation processes are quite recent [8−16] and involve the collection of MALDI spectra at different exposure times to observe the structural changes induced by heat or light under an oxidizing atmosphere. The polymer sample can be then analyzed, and the MALDI spectrum arises from a mixture of pristine and oxidized chains.[8−16]

From the results of the MALDI investigations of photooxidation and thermal-oxidation of polymer systems such as polycarbonate,[8,9] nylon-6,[10,14] nylon-66,[13,15] poly(ether imide)[12]and poly(butylenesuccinate),[16] it appears that unprecedented progress in the current understanding of the oxidation processes occurring in complex macromolecular systems has been achieved.

In the present paper we describe the identification of oligomers produced during the thermal oxidation process of ULTEM[17−19] exposed at 350 °C in the air.

Experimental Section

Materials. Basic materials were commercial products appropriately purified before use. Poly{2,2-bis[4-(3,4-dicarboxyphenoxy)phenyl]propane dianhydride−1,3-phenylendiamine} copolymer (ULTEM) and 2-(4-hydroxyphenylazo)benzoic acid (HABA) were obtained from Sigma-Aldrich Chemical Co (Italy) and used as supplied.

MALDI—TOF Analysis. Matrix assisted laser desorption ionization time-of-flight (MALDI−TOF) mass spectra were recorded in *linear and reflectron mode* using a Voyager-DE STR instrument and in *reflectron mode* by using a Bruker Reflex II. Both instruments are equipped with a nitrogen laser emitting at 337 nm and working in positive ion mode. The accelerating voltage was 20−25 kV, and the grid voltage and delay time (delayed extraction, time lag) were optimized for each sample to obtain the higher molar mass values. The laser irradiance was maintained slightly above threshold. The MALDI−TOF MS-MS analyses were performed by using an Applied Biosystems 4700 Proteoming analyzer equipped with a collision induced decomposition (CID) chamber, using argon as the collision medium.

The resolution of the MALDI spectra reported in the text ranges between 7000 and 18000 full width at half-maximum (fwhm), depending on molar mass distribution, purity and oxidation level of the samples. Mass accuracy, determined by external calibration, was lower than 150 ppm for masses in the range of 1000−2500 Da.

Sample preparation for MALDI analysis involved mixing of adequate volumes of the matrix solution (HABA, 0.1 M in THF/$CHCl_3$) and polymer solution (2 mg/mL in $CHCl_3$) to obtain a 1:1 or 1:3 ratio (sample/matrix, v/v). A solution of sodium trifluoroacetate (NaTFA) or potassium trifluoroacetate (KTFA) (1 μL of 0.1 M) in $CHCl_3$ was added to achieve the type of cationization needed. Eeach sample/matrix mixture 1 μL, was spotted on the MALDI sample holder and slowly dried to allow matrix crystallization.

Deisotoping Procedure. To distinguish and separate among the contributions of isotopic peaks $M + 1$ and $M + 2$

† E-mail: scarroccio@dipchi.unict.it.
‡ E-mail: gmontaudo@dipchi.unict.it.

10.1021/ma0502349 CCC: $30.25 © 2005 American Chemical Society
Published on Web 07/13/2005

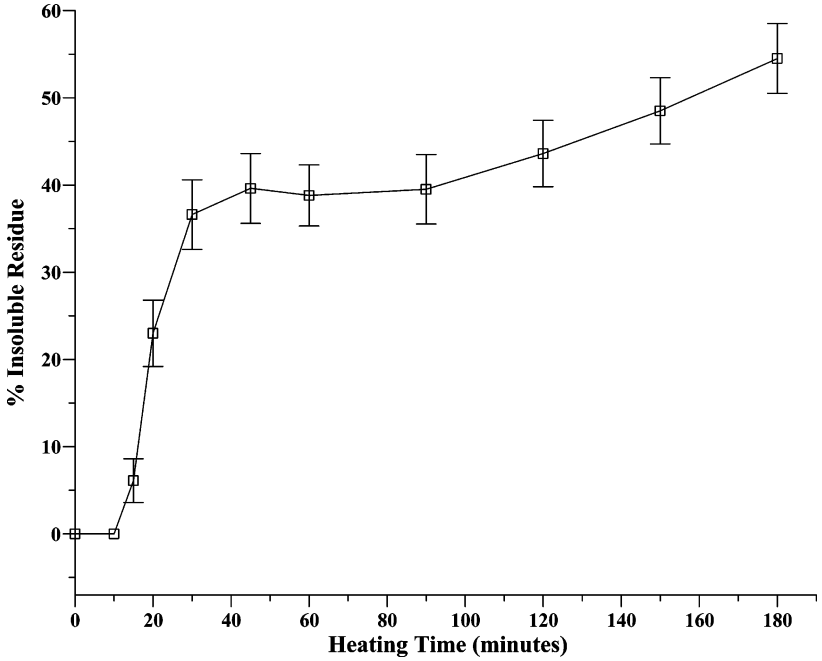

Figure 1. $CHCl_3$ % of insoluble residue from ULTEM as a function of heating time at 350 °C.

and peaks due to isobaric structures, a deisotoping program (Mariner Lab) was used. This program produces a theoretical spectrum corresponding to each structural formula and subtracts from the experimental spectrum the calculated intensity for the $M + 1$ and $M + 2$ isotopic peaks. Thus, the deisotoping spectrum shows only the first mass peak M for each species.

Kinetics. The relative amounts of species monitored in kinetic experiments were obtained as the ratio I_A/I_T, where I_A is the sum of the peak intensity of each species in the mass range 1800−5000 Da and I_T corresponds to the sum of the intensity of all peaks appearing in the same mass range.

Thermooxidative Degradation of ULTEM. The thermooxidative degradation was carried out on 10 μm films of ULTEM in the presence of air at 350 °C. ULTEM samples were placed in a glass vessel and reacted for 15, 30, 60, 90, and 180 min, respectively. The oxidized samples were dissolved in $CHCl_3$, and the soluble portions were analyzed by MALDI−TOF.

Results and Discussion

ULTEM films were heated at 350° C in atmospheric air for up to 180 h. At this stage the samples formed about 50% insoluble residue (Figure 1). The concomitant polymer degradation and extensive cross-linking cause uncertainty in the average molar mass determination. In fact M_n and M_w values of the soluble ULTEM portion do not show a detectable change as a function of exposure time. The exposed samples were filtered, to generate a soluble portion suitable for MALDI analysis. Attempts to obtain MALDI spectra of the insoluble residue by solvent free techniques[21] were unsuccessful, as were attempts to hydrolyze or aminolyze the charred residue.

This is not surprising, since polymers containing aromatic units in their repeat unit tend to form a charred residue with quasi-graphite structure and become quickly intractable. Several bridged polyaromatics such as PPO, PES and PEK,[22] PPS,[23] and poly(xylilene sulfide)[24] show a marked tendency to produce a graphitelike pyrolysis residue.

In the case of BPA−polycarbonate (PC), thanks to the easily cleavable carbonate units, it was possible to aminolyze the insoluble pyrolysis residue, and the MS analysis showed that it is constituted of thermal rearranged sequences which undergo aromatization and cross-linking processes, leading to a graphitelike charred residue as the temperature increases.[25]

Hydrolysis of the insoluble residue and subsequent MALDI analysis was also successfully performed for Ny66, but that polymer possesses an aliphatic structure.[13]

The MALDI spectrum of the original ULTEM has been already reported,[12] and therefore, only expanded portions in the mass range 1800−2400 Da are presented here.

The MALDI spectrum of the unexposed sample, reported in Figure 2a, shows peaks belonging to six different mass series, corresponding to sodiated macromolecular ions.

The most intense peaks in Figure 2a are due to cyclic oligomers at m/z 1801+ n592.6 Da (mass series A, Table 1), whereas at higher molar masses the most prominent peaks appear at m/z 2169+ n592.6 Da (mass series B, Table 1), corresponding to oligomers with phenylphthalimide end groups at both ends.

A third mass series, appearing in Figure 2a at m/z 1949+ n592.6 Da, can be assigned to oligomers of type C, Table 1, corresponding to sodiated ions terminated with phenylphthalimide at one end and phthalic anhydride groups at the other end.

The fourth mass series at m/z 1962 + n592.6 Da corresponds to macromolecular ions bearing phenylphthalimide at one end and *N*-methylphthalimide terminal groups at the other end (mass series D, Table 1).

The last two peaks series, appearing with low intensity in Figure 2a, are due, respectively, to macromolecular ions with *N*-methylphthalimide end groups (mass series F, Table 1), and to *N*-methylphthalimide/phthalic anhydride terminal groups (mass series E, Table 1).

From the inspection of the spectra in Figure 2b−c, it is possible to observe a detectable increment of peaks with respect to the blank sample in Figure 2a. This indicates that thermooxidation reactions have occurred

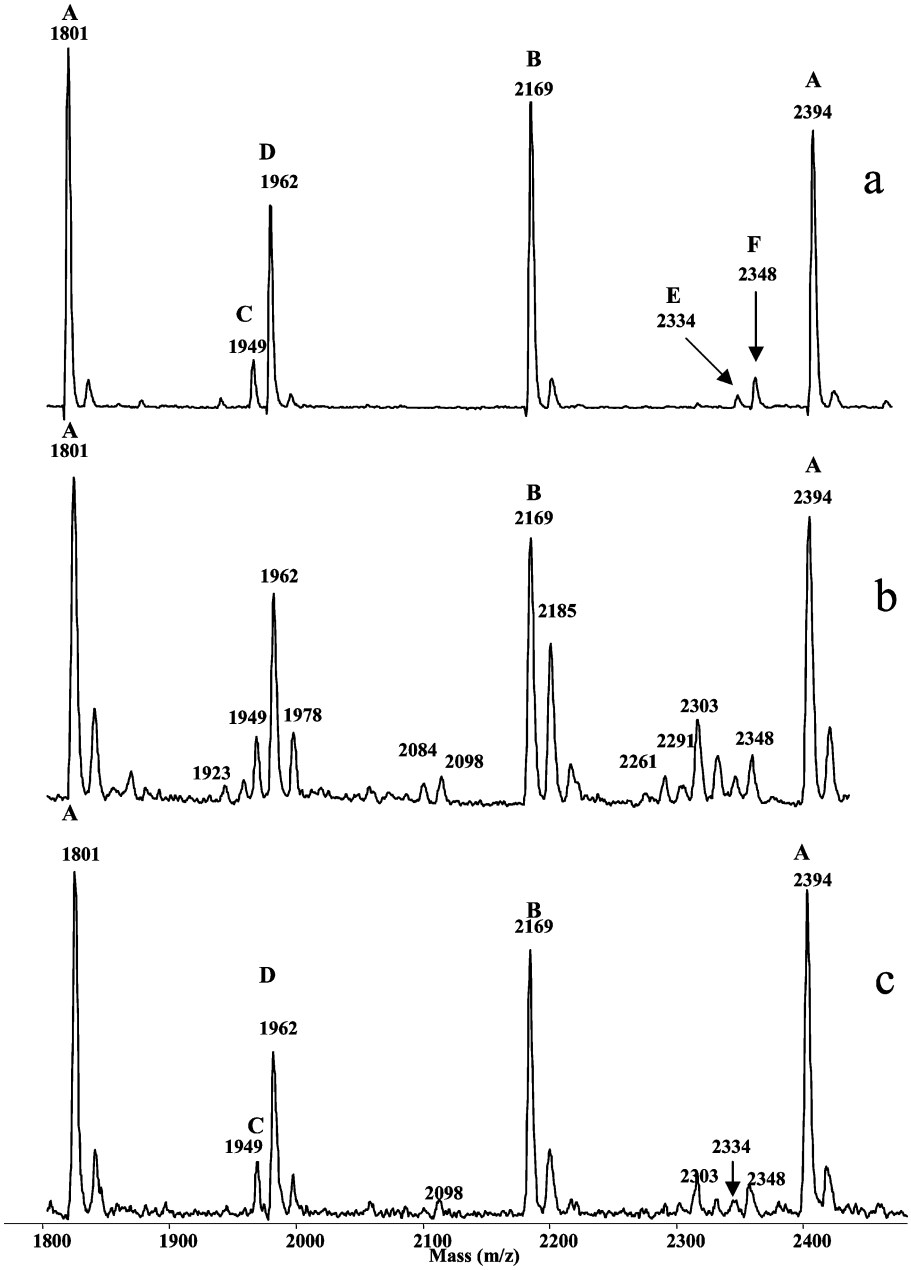

Figure 2. MALDI−TOF spectra in the mass range 1800−2400 Da of ULTEM samples oxidized at 350 °C for 0 (a), 30 (b), and 180 min (c).

in ULTEM, producing new compounds that are detected and differentiated by the MALDI analysis.

The spectra sequence (Figure 2a−c) permits the evolution of the oxidation process to be followed. The amount of oxidized species present in the sample heated for 180 min appears lower with respect to the sample heated for 30 min, and this result may appear contradictory.

However, the decrement of oxidized species with time is only apparent, being related to the intervening cross-linking phenomena in the oxidation process. In fact, the cross-linked fraction (which contains a major portion of the oxidized products) becomes insoluble and cannot be detected, because MALDI analyzes only the soluble material.[8]

The kinetics of the oxidation process is shown in Figure 3, in which the relative amount of some species (Tables 1 and 2) is reported as a function of the heating time. The rapid depletion of species B, the linear oligomers present in the unexposed polymer, and the correlated increment of some species produced in the thermal oxidation process are noted.

Because of the relatively low resolution of the MALDI spectra in Figure 2b,c (recorded in linear mode), the identity and relative intensity of several peaks are not easily assessed. As discussed above (see Experimental Section), the MALDI spectra were also obtained by using the MALDI instrument *in reflectron mode* that allows achieving peak isotopic resolution.

Therefore, the spectrum (region 1000−5500 Da) of the unexposed ULTEM sample, obtained in reflectron mode (resolution 18000 fwhm), with an accuracy of 140 ppm at 1800 Da is reported in Figure 4. The inset in Figure 4 displays an expanded portion of the peaks in the region 1800−2400 Da, which show well-resolved isotopic distribution profiles. Peaks assignments are reported in Table 1.

Table 1. Structural Assignments of Ions Appearing in the MALDI−TOF Spectra of the Original ULTEM Sample

Series Mass	Oligomer Structures	M Na^+	M K^+
A	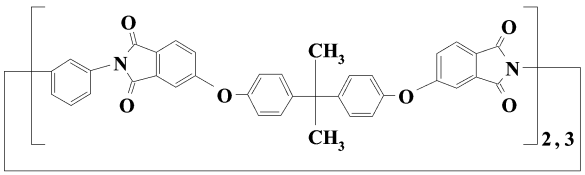	1207.3 1799.5	1223.3 1815.4
B	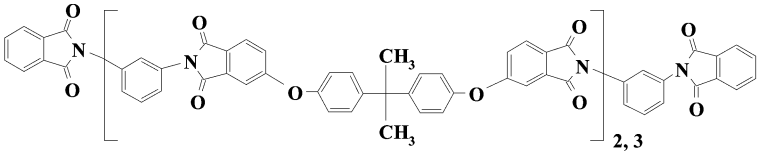	1575.4 2167.5	1591.4 2183.5
C	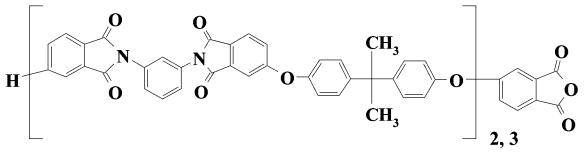	1355.3 1947.5	1370.3 1962.5
D	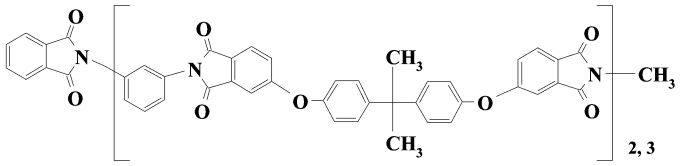	1368.4 1960.5	1384.3 1976.5
G	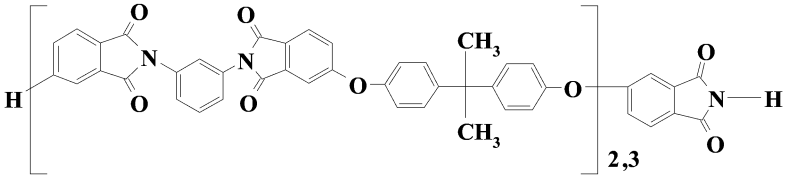	1355.4 1946.5	
E	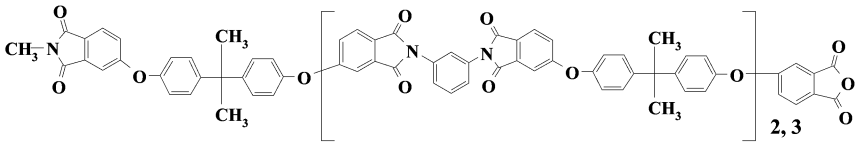	1740.5 2332.6	
F	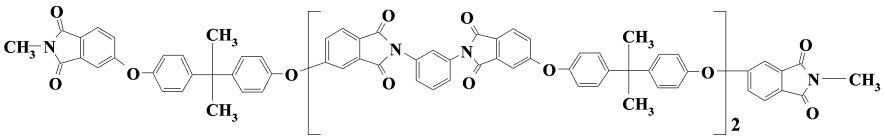	1753.5 2345.6	

The spectrum (region 1000−8000 Da) of the ULTEM sample heated for 120 min at 350 °C, obtained in reflectron mode with a resolution of 8000 Da, is reported in Figure 5. The inset in Figure 5 displays an expanded portion of the peaks in the region 1800−2400 Da, showing the presence of numerous new peaks with well-resolved isotopic distribution profiles.

The isotopic distribution profiles of all the peaks falling in the region 1200−2400Da are reported in Figures 1Sa−l. Peak assignments are reported in Table 2.

It should be noted that the latter can result a demanding task, because the MALDI spectra of complex molecules may present several peaks that could correspond to isobaric or quasi isobaric structures.

Both the analysis of isotopic distribution profiles and the deisotoping procedure, help considerably in the peak-assignment process (see Experimental Section). Furthermore, a tool frequently used in the peak assignment task is the effect of doping agents, in fact the doping procedure is able to help in the presence of isobar structures.[26]

The comparison between the MALDI spectra, b and d, obtained upon adding potassium salt and spectra a and c, obtained without addition of a specific cationizing reagent salt, is reported in Figure 6.

In Table 1, the peaks at 1207.3 and 1223.3 Da have been assigned to a cyclic oligomer desorbing as sodiated and potassiated adducts, as shown in Figure 6a. An alternative structural assignment for the peak at 1223.3

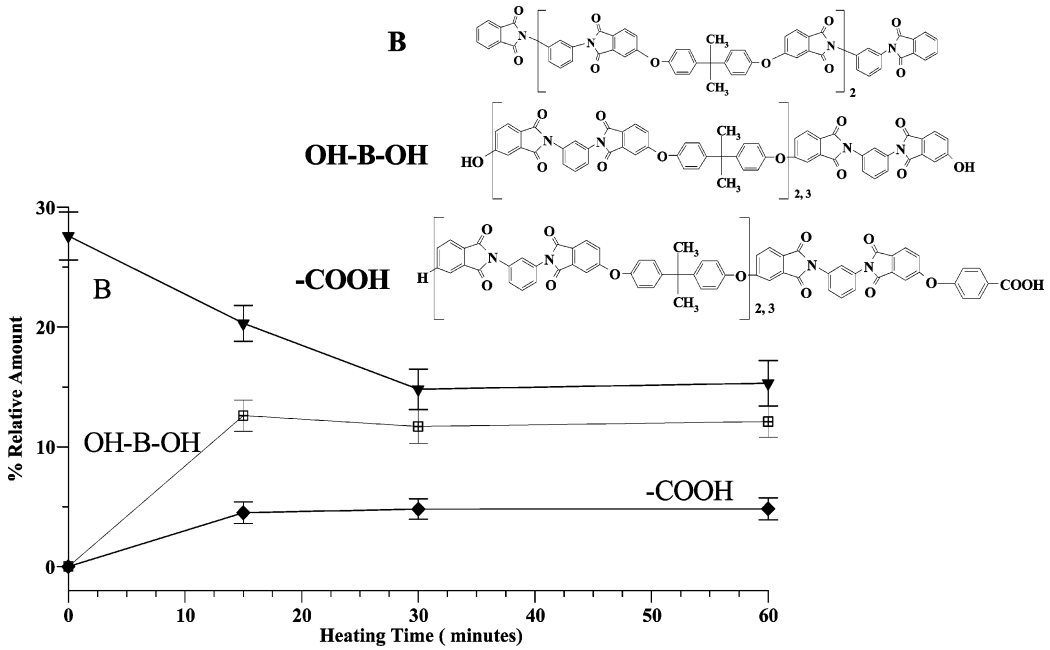

Figure 3. Relative amount vs heating time of species B at *m/z* 1575.5: (a, b) OH−B−OH at *m/z* 1607.4 and (c) −COOH at *m/z* 1711.5 as obtained from the MALDI spectra of oxidized ULTEM sample at 350 °C.

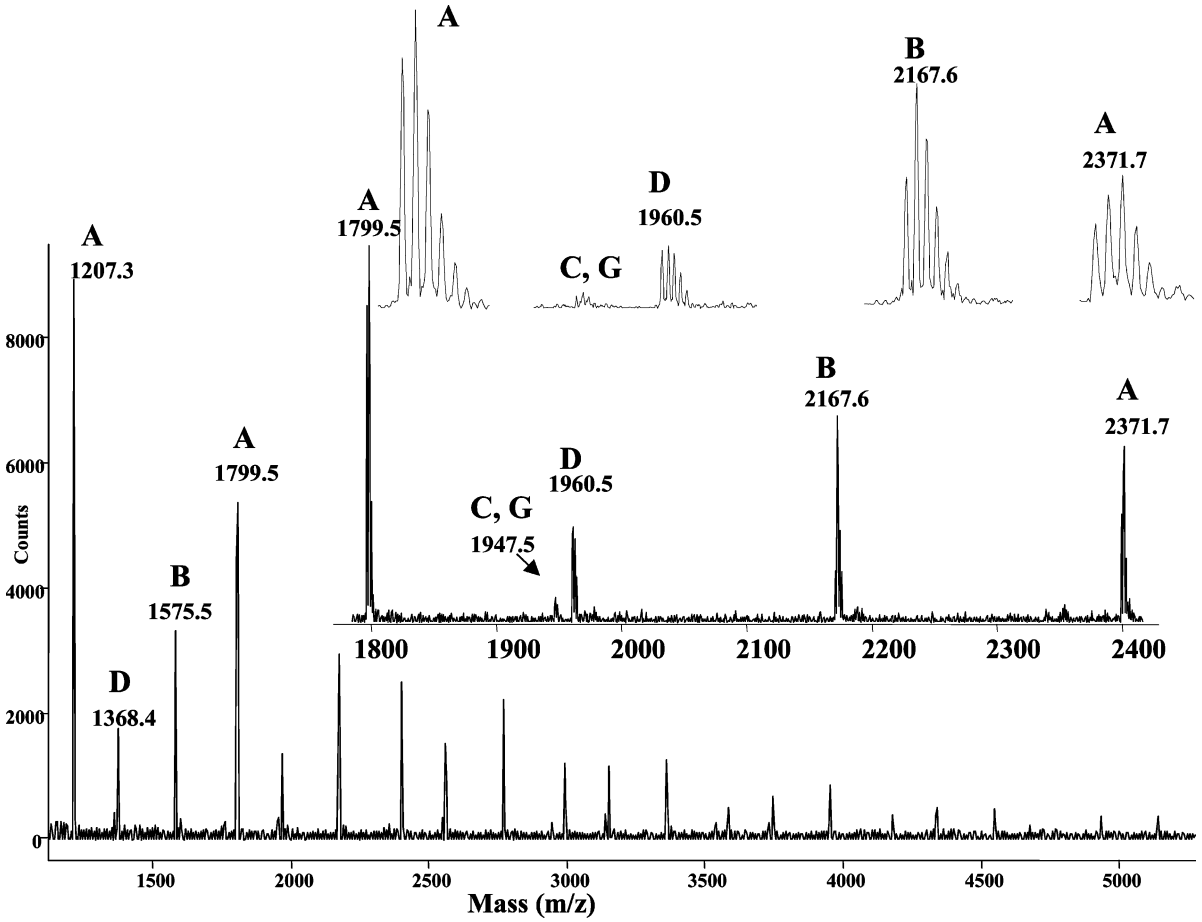

Figure 4. MALDI−TOF mass spectrum obtained in reflectron mode of the original ULTEM sample.

Da might be a new product obtained by oxidation. However, in the potassium-doped spectrum (Figure 6b), the desorption of the sodiated species is completely suppressed and the spectrum shows a single signal due to the potassiated compound, and the appearance of an additional peak of the potassiated species is not noticed. This observation allows the univocal assignment of the two signals appearing in Figure 6a to sodiated and potassiated adducts of the cyclic oligomer in Table 1.

Analogously, Figure 6c shows a portion of the undoped spectrum where four signals at 16 mass units distance from each other, which may belong to several isobaric structures (Tables 1 and 2) are present. In particular, it is not possible to discriminate between species B K^+

Table 2. Structural Assignments of Ions Appearing in the MALDI−TOF Spectra of the ULTEM Oxidized Sample at 350 °C

Structures	M Na^+	M K^+	Decomposition processes
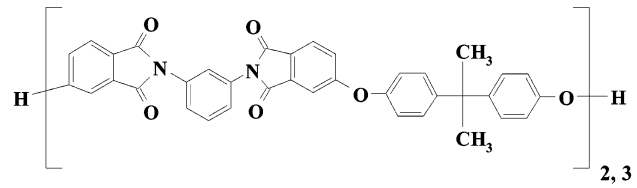	1209.3 1801.5		T2-T2
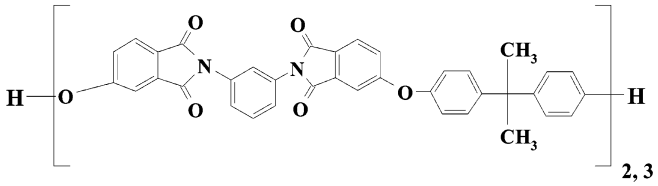			T1-T1
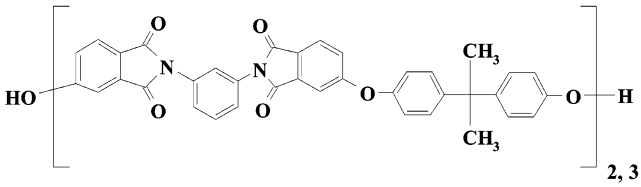	1225.3 1817.5	1241.3 1833.5	T1-T2
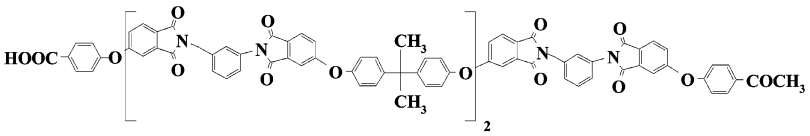	1253.4 1845.5	1269.4 1861.5	T3-T3
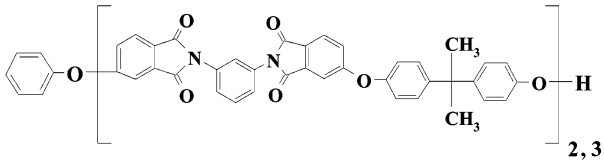	1301.4 1893.5	1317.3 1909.5	T3-T2
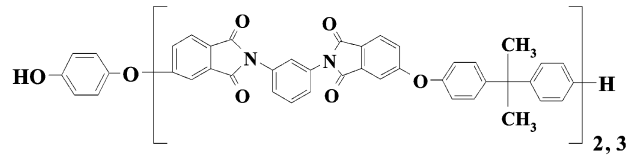			T3-T1
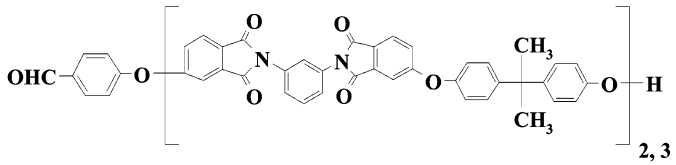	1329.4 1921.5	1345.4 1937.5	T3-T2
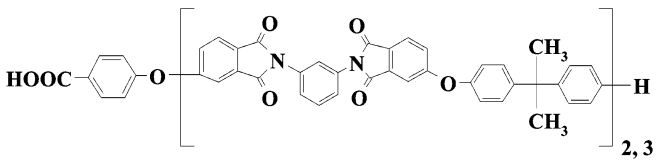			T3-T1
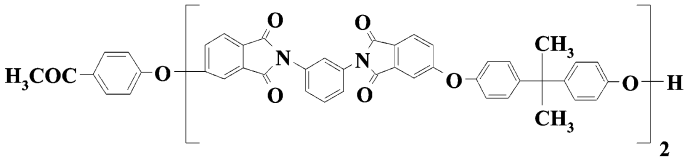	1343.4 1935.5		T3-T2

Table 2 (Continued)

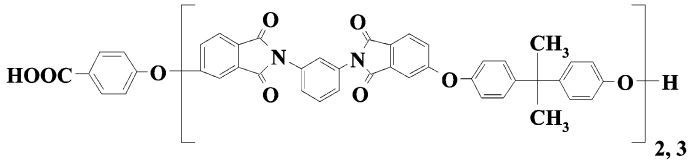	**1345.4 1937.5**		**T3-T2**
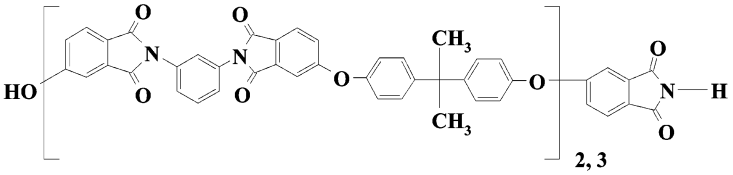	**1370.4 1962.5**		**T1-T4**
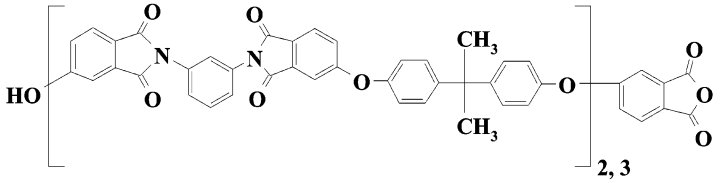	**1371.3 1963.5**		**T1-T4**
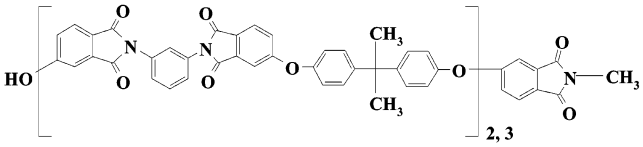	**1384.4 1976.5**	**1400.4 1992.5**	**T1-E**
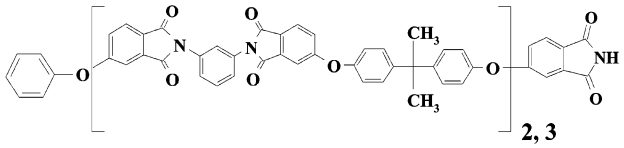	**1446.4 2038.5**		**T3-T4**
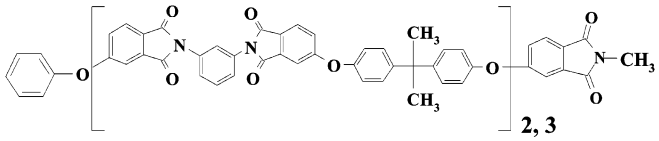	**1460.4 2039.5**		**T3-E**
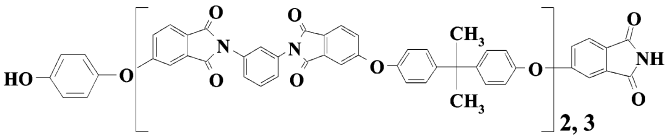	**1462.4 2054.5**		**T3-T4**
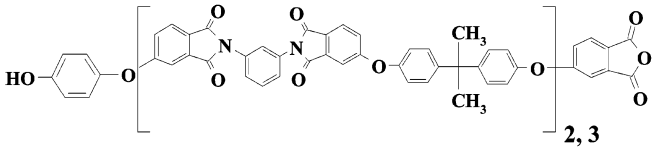	**1463.4 2055.5**		**T3-T4**
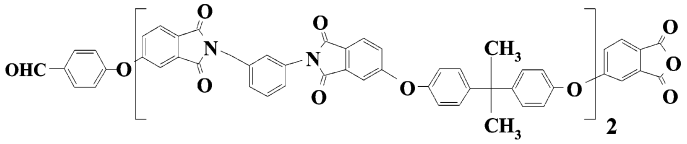	**1475.4 2067.5**		**T3-T4**
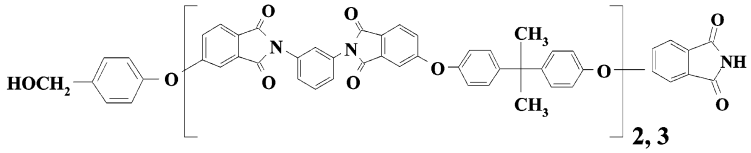	**1476.4 2068.5**		**T3-T4**

Table 2 (Continued)

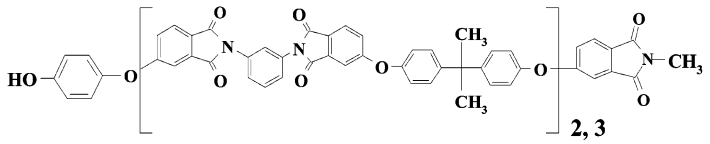	**1476.4 2068.5**		**T3-E**
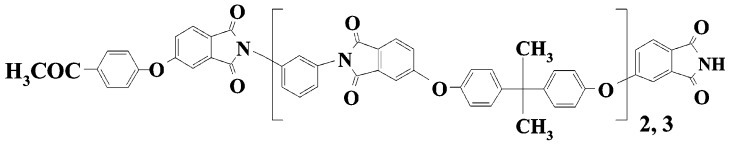	**1488.4 2080.6**		**T3-T4**
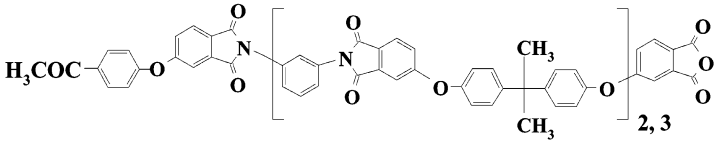	**1489.4 2081.5**		**T3-T4**
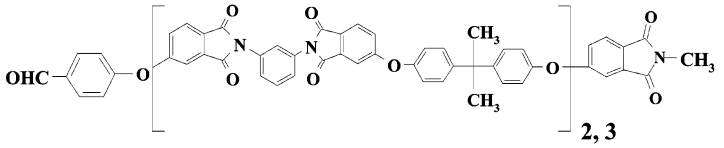	**1488.4 2080.6**		**T3-E**
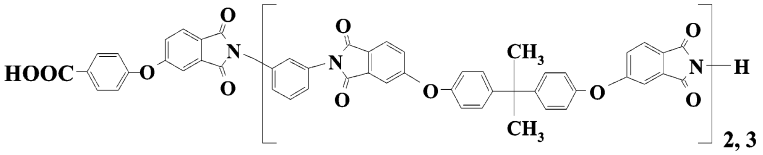	**1490.4 2082.5**		**T3-T4**
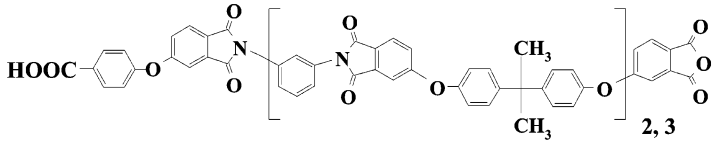	**1491.4 2083.5**		**T3-T4**
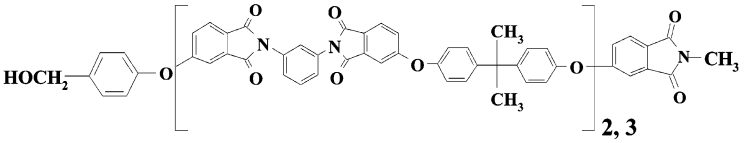	**1490.4 2082.6**		**T3-E**
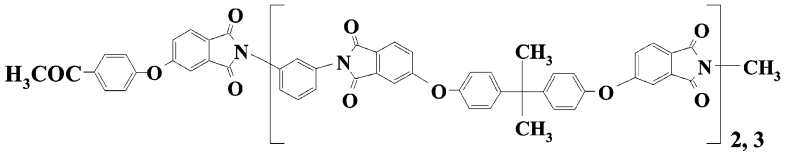	**1502.4 2094.6**		**T3-E**
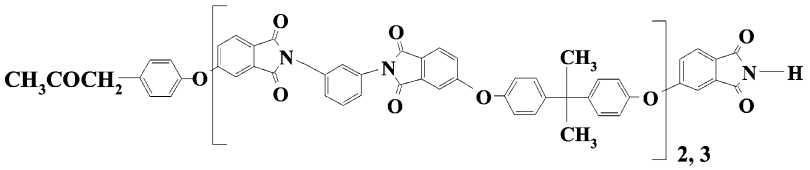	**1502.4 2094.6**		**T3-T4**
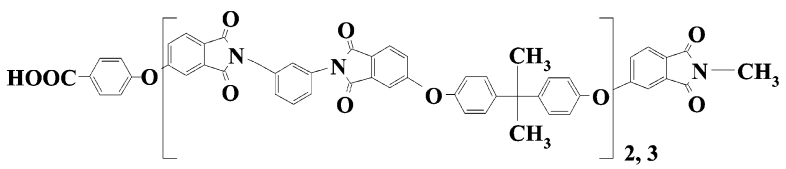	**1504.4 2096.5**	**1520.4**	**T3-E**

Table 2 (Continued)

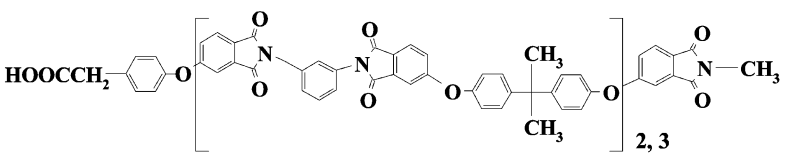	**1518.4 2110.6**		**T3-E**
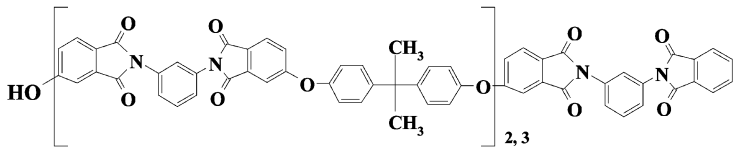	**1591.4 2183.5**		**T1-T2**
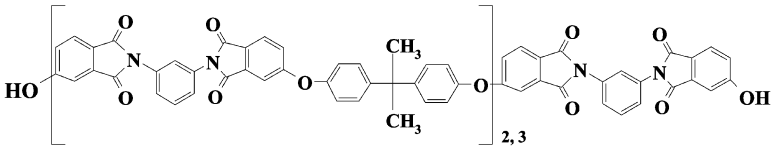	**1607.4 2183.5**		**T1-T1**
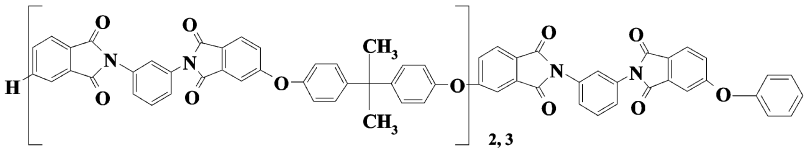	**1667.4 2259.6**		**T2-T3**
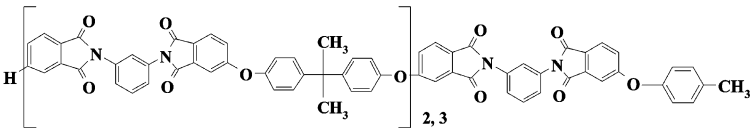	**1681.4 2273.6**		**T2-T3**
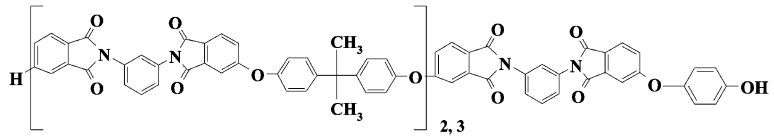	**1683.4 2275.6**		**T2-T3**
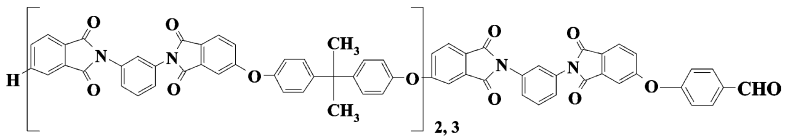	**1695.4 2287.6**		**T2-T3**
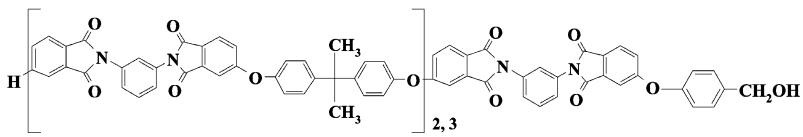	**1697.4 2289.6**		**T2-T3**
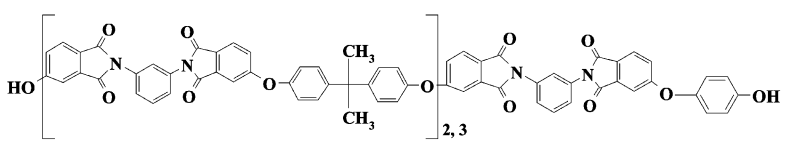	**1699.4 2291.6**		**T1-T3**
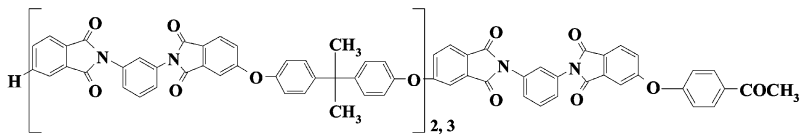	**1709.4 2301.6**		**T2-T3**
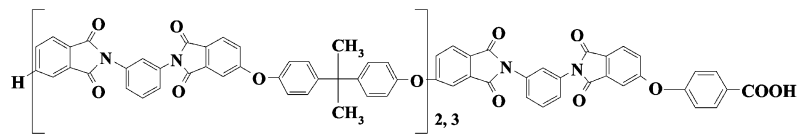	**1711.4 2303.6**		**T2-T3**

Table 2 (Continued)

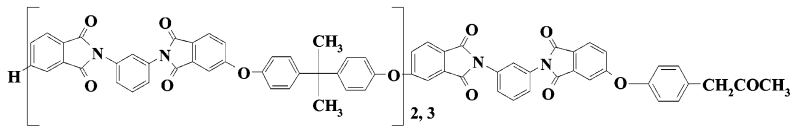	**1723.4** **2315.6**		**T2-T3**
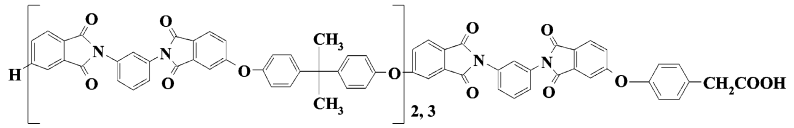	**1725.4** **2317.6**		**T2-T3**
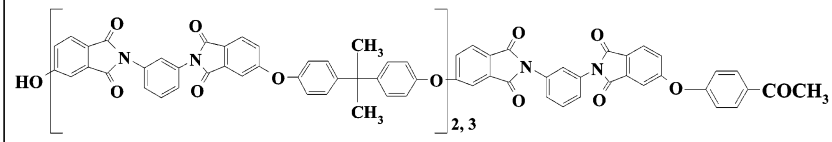	**1725.4** **2317.6**	**1741.5**	**T1-T3**
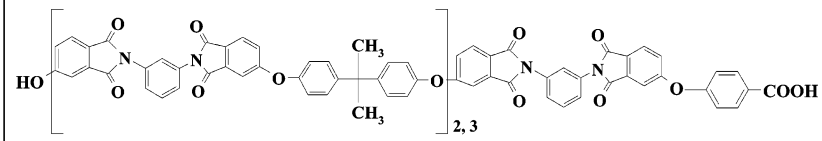	**1727.4** **2319.6**		**T1-T3**
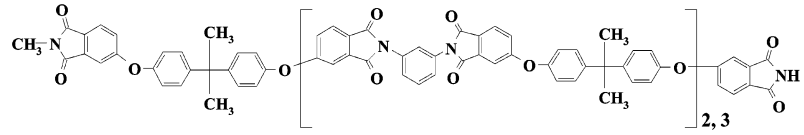	**1739.5** **2331.6**		**E-T4**

and B−OH Na^+ (1591.4 Da) and between species B−OH K^+ and HO−B−OH Na^+ (1607.4 Da).

However, in the potassium-doped spectrum (Figure 6d), where the sodiated species at 1575.4 Da is completely suppressed, the spectrum shows three signals due to the potassiated compound.

This result allows the univocal assignment of the two signals at 1591.4 and 1607.4 Da to the oxidation products BOH and to BOHOH.

In Figure 7a,b the spectrum of the unexposed ULTEM sample and that of the sample heated for 120 min at 350 °C, shown as they appear after the deisotoping

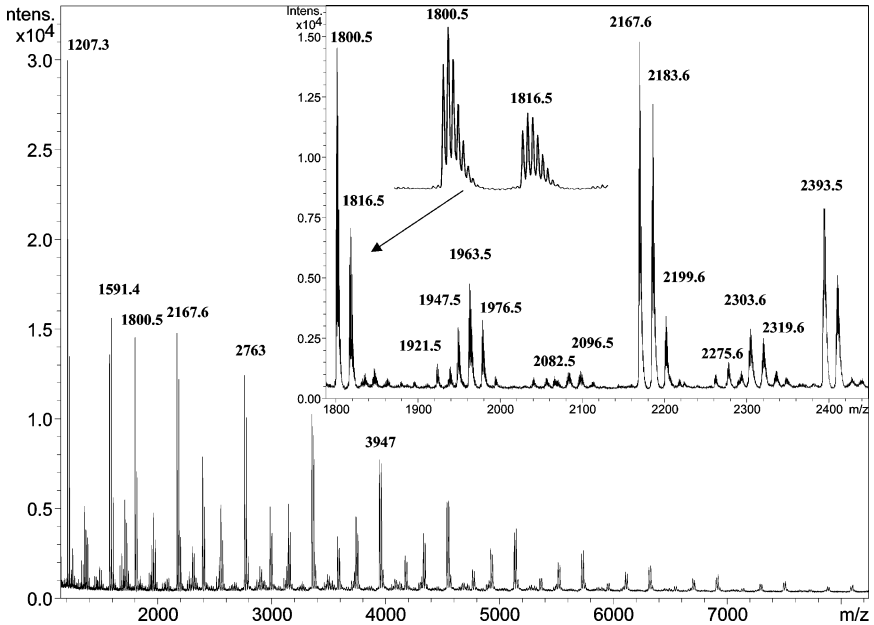

Figure 5. MALDI−TOF spectrum obtained in reflectron mode, in the mass range 1800−8000 Da of the oxidized ULTEM sample at 350 °C for 120 min.

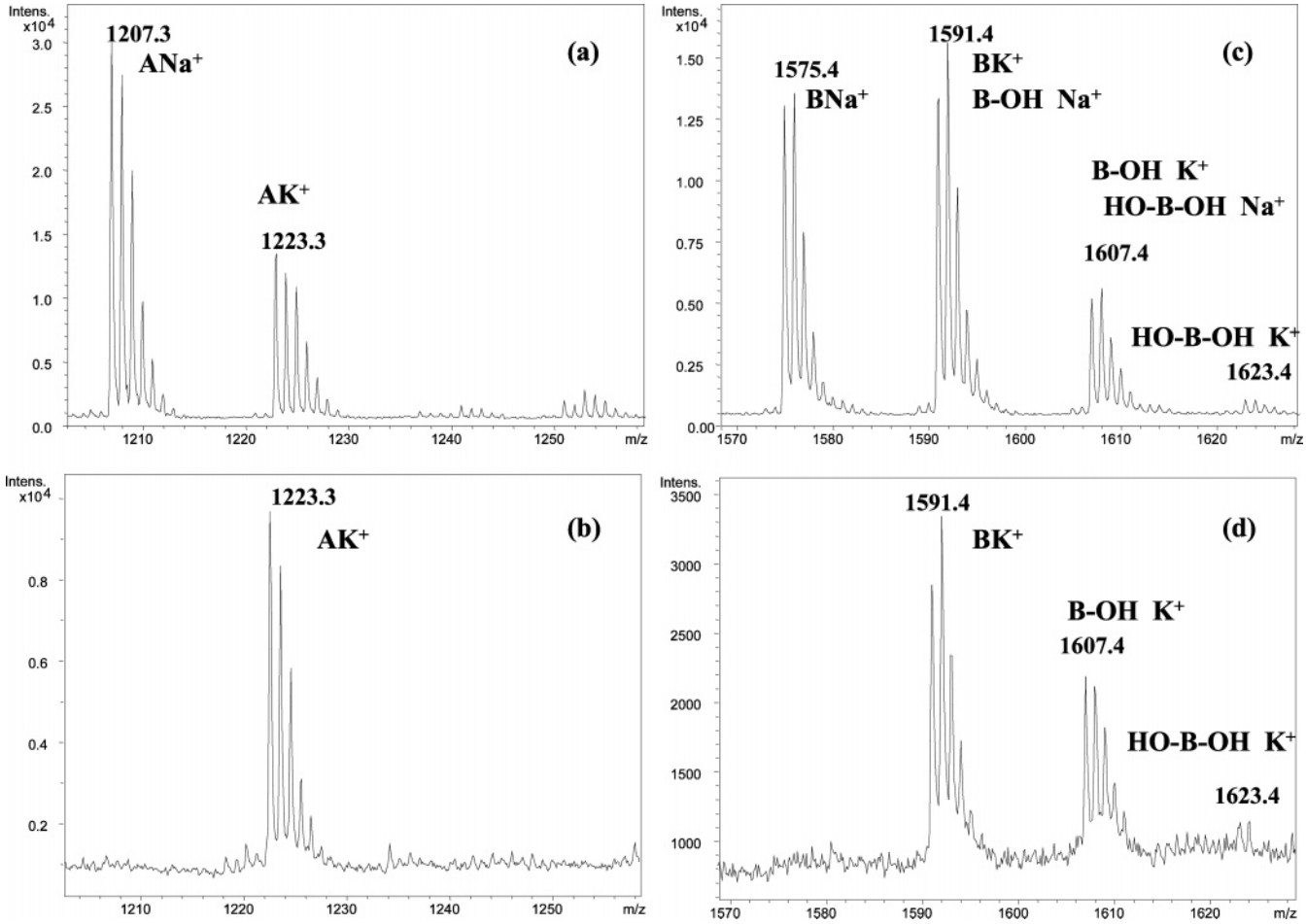

Figure 6. Comparison of cycle (a) and B peaks (c) obtained after total cationization with potassium salt (b and d).

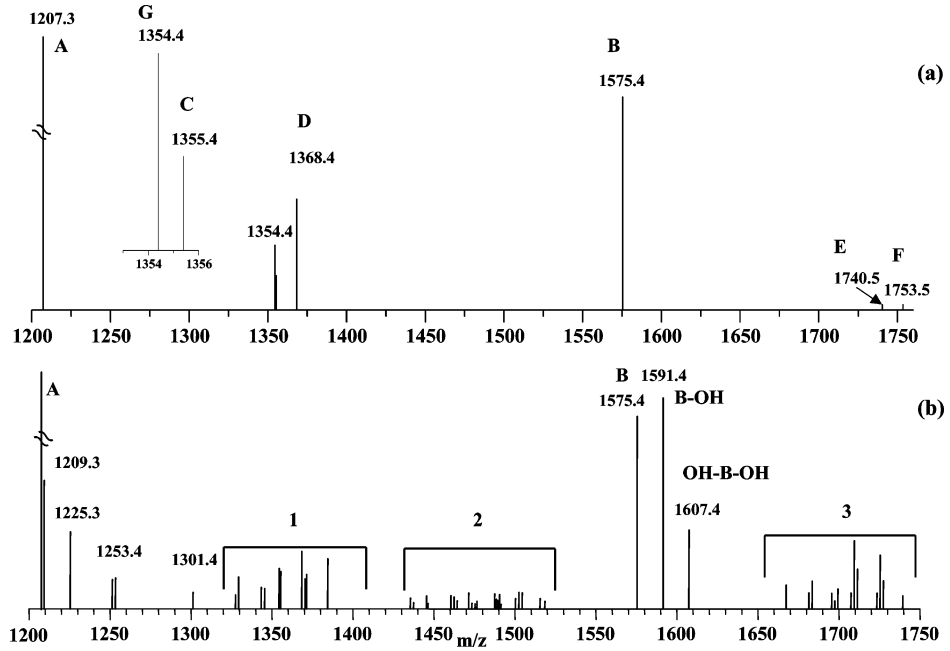

Figure 7. Deisotoping MALDI−TOF mass spectra in the mass range of 1200−1750 Da of the original ULTEM sample (a) and the sample oxidized for 120 min at 350 °C (b).

procedure,[14−16] are reported. Figure 8 reports a further expansion of the deisotoping spectrum of the ULTEM sample heated for 120 min at 350 °C.

Over 40 new oligomers are present in the mass spectrum of the oxidized sample, as compared to only seven in the original ULTEM sample. All these peaks correspond to sodiated ions of oxidized ULTEM oligomers, and they have been assigned (Table 2) to oligomers containing ULTEM repeat units terminated by different end groups.

The structural identification of end groups attached to the oligomers produced in the oxidation process

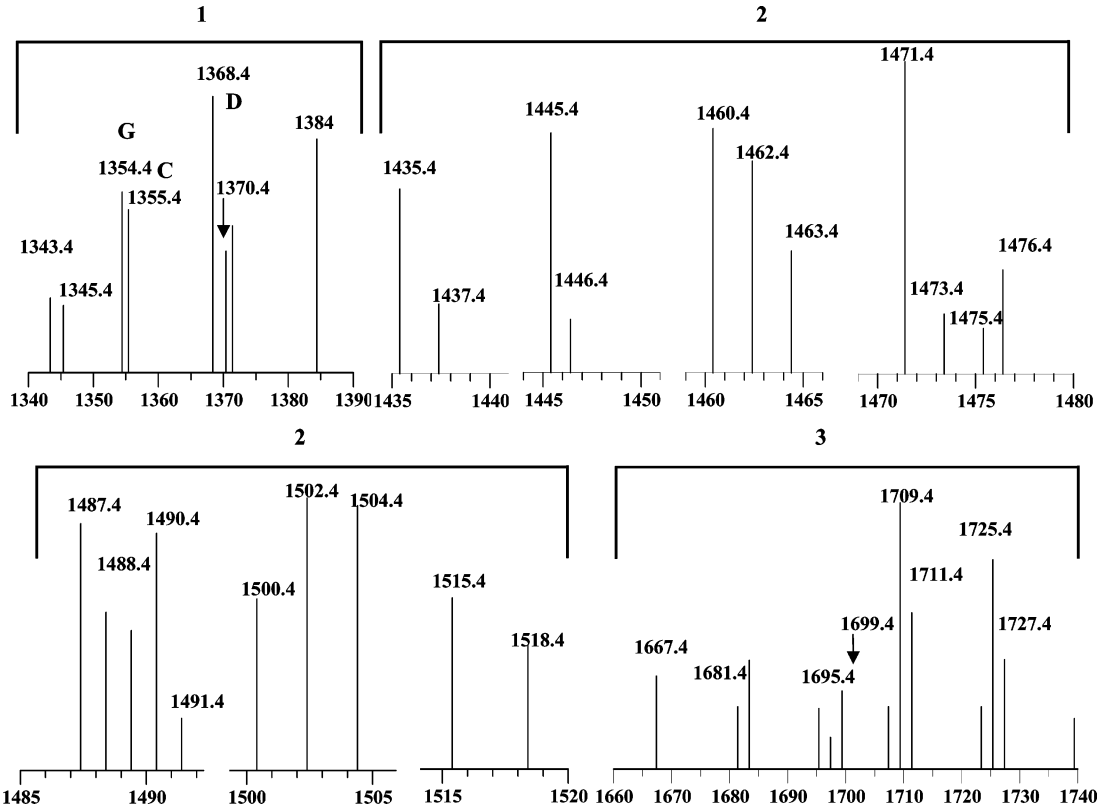

Figure 8. Expanded portions of the deisotoping MALDI spectrum of the ULTEM sample oxidized at 350 °C for 120 min.

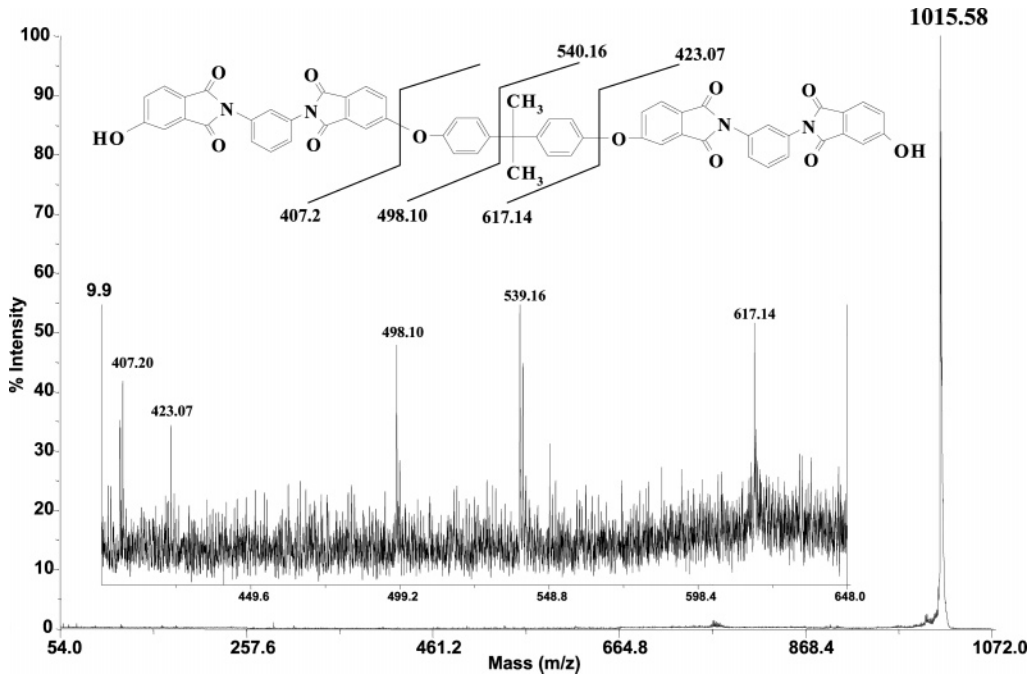

Figure 9. MALDI−TOF−TOF spectrum of peak at *m/z* 1015.6 from the ULTEM sample oxidized for 2 h at 350 °C.

(Figures 5−8, Table 2) is revealing, because the end groups are related to the particular oxidation mechanism.

Going into a detailed analysis of the data in Figures 7 and 8, apart from peaks A and B, representing the pristine cyclic and linear ULTEM oligomers, the most intense peaks in Figure 7b appear at 1591.4 and 1607.4 Da. They have been assigned to oligomers terminated by one or two hydroxyl groups attached to phthalimide units (B−OH, HO−B−OH, Table 2). Weaker peaks of the same type are found at 1370.4, 1371.3, and 1384.4 Da (Table 2).

This particular structural assignment is crucial to establish the oxidation mechanism and was confirmed by the MS/MS analysis of the oligomer at 1015.58 Da. The collision-induced decomposition MALDI−TOF spectrum (see Experimental Section) of this oligomer is reported in Figure 9, and the structures of the

Scheme 1. Overall Thermooxidative Processes in ULTEM

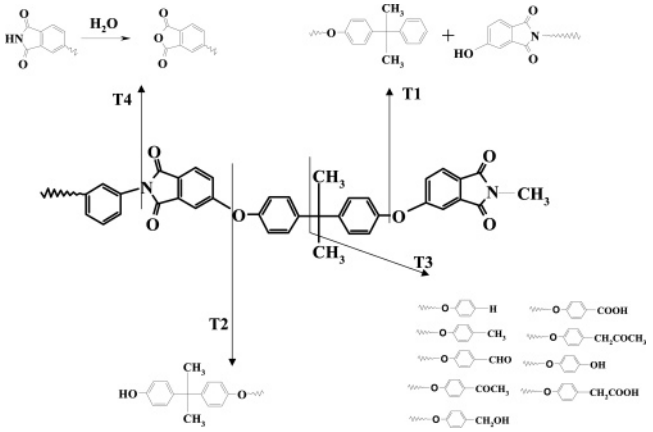

ion fragments produced, also shown in Figure 9, correspond to those expected for an oligomer terminated by two hydroxyl groups attached to phthalimide units.

Peaks corresponding to oligomers terminated by Bisphenol A units (and therefore bearing hydroxyl ends, Table 2) are also found in the expanded portions reported in Figure 7 at 1301.4, 1329.4, 1343.4, and 1345.4 Da. The first two oligomers are isobar with structures bearing phenyl/phenol end groups and phenyl/benzoic acid groups, as also indicated in Table 2.

In Table 2 also appear several oligomers at 1253.4, 1476.4, 1488.4, 1490.4 1502.4, 1504.4, 1518.4, Da, whose structures are assigned in Table 2, generated by the oxidative cleavage of the BPA isopropylidene bridge (see below) are also apparent.

From the results obtained, four processes may be hypothesized to occur in the thermal oxidation of ULTEM at 350°C (Scheme 1): (i) thermal cleavage of the diphenyl ether units (T_1 in Scheme 1), to yield oligomers with 3-hydroxyphthalimide end groups plus oligomers with phenyl end groups; (ii) thermal cleavage of the diphenyl ether units (T_2 in Scheme 1), to yield Bisphenol A end groups; (iii) thermal oxidative degradation of the isopropylidene bridge of BPA units (T_3 in Scheme 1) to yield benzyl alcohol, acetophenone, phenyl-substituted acetone, phenylacetic acid, phenol, benzoic acid end groups; (iv) thermal cleavage of phenyl-phthalimide units (T_4 in Scheme 1) to yield phthalimide and phthalic anhydride end groups.

In Table 2, beside the structural assignments, the decomposition pathway that is responsible for the formation of each new oligomer produced in the thermal oxidation process is specified.

We have adopted a code to specify the relationship between each oligomer end group and the thermal oxidation mechanism from which it originated.

Thus, the symbol T_1 specifies the decomposition of the diphenyl ether units to yield 3-hydroxyphthalimide end groups (Scheme 1); symbol T_2 specifies the thermal cleavage of the diphenyl ether units to yield Bisphenol A end groups; symbol T_3 specifies the thermal oxidative degradation of the isopropylidene bridge of BPA units to yield benzyl alcohol, acetophenone, phenyl-substituted acetone, phenyl acetic acid, phenol and benzoic acid end groups; symbol T_4 specifies the thermal cleavage of phenylphthalimide units to yield phthalimide and phthalic anhydride end groups, whereas symbol E

Scheme 2. Thermal Oxidation Process Occurring in the Bisphenol-A Unit

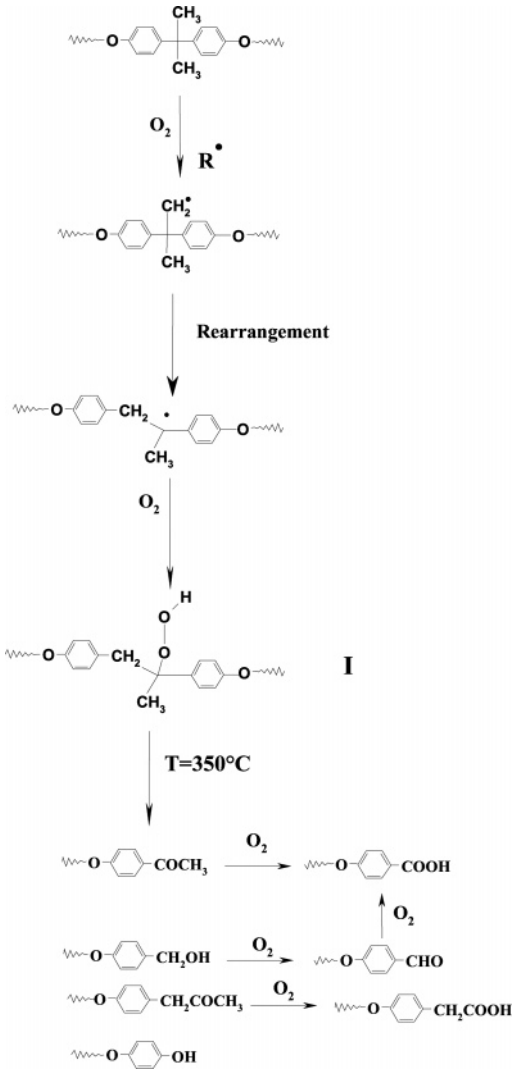

indicates just one of the end groups present in the original ULTEM sample (Table 1).

Because each oligomer has two ends, the notation T_1-T_4, for instance, means that a chain cleavage process involving the decomposition of diphenyl ether units to yield 3-hydroxy phthalimide end groups occurred at one end, whereas the cleavage of phenylphthalimide units to yield phthalimide and phthalic anhydride end groups occurred at the other end.

Remarkably, only the process T_3 (Scheme 1) corresponds to a pure thermooxidation reaction of ULTEM, whereas the degradation pathways T_1, T_2, and T_4 are pure thermal scissions.

In fact, the formation of the compounds related to these cleavage pathways was already detected when studying the thermal degradation of ULTEM in an inert atmosphere.[27]

On the contrary, process T_3 corresponds to the thermal oxidative degradation of the isopropylidene bridge of BPA units.

The latter process occurs as described in detail in Scheme 2, and the production of all the end groups observed here has been also found in a study of the thermooxidative degradation of BPA−polycarbonate.[8] All the end groups predicted by this reaction scheme have been detected in the MALDI spectra discussed above.

Acknowledgment. Partial financial support from the Italian Ministry for University and for Scientific and Technological Research and from the National Council of Research (CNR, Rome) is gratefully acknowledged. We are grateful to Dr. Dietmar Waidelich and Dr. Matthias Glueckmann (Applied Biosystems) for MALDI−TOF MS/MS spectra; to Dr. Marco Biglietto (Applied Biosystems) and Dr. Domenico Garozzo (CNR ICTP, Catania, Italy) for their support and suggestions.

Supporting Information Available: Figure 1S. MALDI−TOF mass spectra of ULTEM samples oxidized at 350 °C for 2 h in the mass ranges (a) 1200−1300, (b) 1310−1410, (c) 1440−1530, (d) 1570−1630, (e) 1660−1770, (f) 1790−1870, (g) 1900−2010, (h) 2020−2130, (i) 2140−2240, and (l) 2250−2380 Da. This material is available free of charge via the Internet at http://pubs.acs.org.

References and Notes

(1) Samperi, F.; Montaudo, M. S.; Montaudo, G. *Mass Spectrometry of Polymers*; Montaudo, G., Lattimer, R. P., Eds.; CRC Press LLC, Boca Raton, FL, 2001; Chapter 10.
(2) Hanton, S. D. *Chem. Rev.* **2001**, *101*, 527−569.
(3) Montaudo, G.; Garozzo, D.; Montaudo, M. S.; Puglisi, C.; Samperi, F.; *Macromolecules*, **1995**, *28*, 7983−7989.
(4) Hawkins, L. *Polym. Degr. Stab.* **1984**.
(5) Factor, A. In *Polymer Durability. Degradation, Stabilization, and Lifetime Prediction*; Clough, R. L., Billingham, N. C., Gillen, K. T., Eds.; Advances in Chemistry 249, American Chemical Society: Washington, DC, 1996, and references therein.
(6) Factor, A.; Chu, M. L. *Polym. Degr. Stab.* **1980**, *2*, 203.
(7) Hoyle, C. E.; Anzures, E. T.; Subramanian, P.; Nagarajan, R.; Creed, D. *Macromolecules* **1992**, *25*, 6651−6657.
(8) Carroccio, S.; Puglisi, C.; Montaudo, G. *Macromolecules* **2002**, *35*, 4297−4305.
(9) Carroccio, S.; Samperi, F.; Puglisi, C.; Montaudo, G. *Macromolecules* **1999**, *32*, 8821−8828.
(10) Chionna, D.; Samperi, F.; Puglisi, C.; Turturro, A.; Montaudo, G. *Macromol. Rapid Commun.* **2001**, *22*, 524−529.
(11) Carroccio, S.; Rizzarelli, P.; Gallet, G.; Karlsson, S. *Polymer* **2002**, 43, 1081−1094.
(12) Carroccio, S.; Puglisi, C.; Montaudo, G. *Polym. Degr. Stab.* **2003**, *80*, 459−456.
(13) Di Giorgi, S.; Samperi, F.; Pulgisi, C.; Montaudo, G. *Polym. Degr. Stab.* **2002**, 78, 369−378.
(14) Carroccio, S.; Puglisi, C.; Montaudo, G. *Macromolecules* **2003**, *36*, 7499−7507.
(15) Carroccio, S.; Puglisi, C.; Montaudo, G. *Macromolecules* **2004**, *37*, 6037−6049.
(16) Carroccio, S.; Puglisi, C.; Montaudo, G. *Macromolecules* **2004**, *37*, 6576−6586.
(17) Takekoshi, T.;.Kochanowski J. S.;. Manello J. S.; Webber M. J. *Polym. Sci. Polym. Symp.* **1986**, *74*, 93−108.
(18) Takekoshi, T.; Kochanowski J. S.; Manello.; Webber M. J. *J. Polym. Sci., Polym. Chem. Ed.* **1985**, *23*, 1759−1769.
(19) Bessonov, M. I.; Koton, M. M.; Kudryavtsed, V. V.; Laius, L. A. *Polyimides*; Plenum Publishing Corporation: New York, 1987.
(20) Carroccio, S.; Puglisi, C.; Montaudo, G. *Macromolecules*, submitted for publication.
(21) Trimpin, S.; Grimsdale, H.; Rader, H. J.; Mullen, K. *Anal. Chem.* **2002**, *74*, 3777−3782.
(22) Samperi, F.; Rapisardi, R.; Puglisi, C.; Montaudo, G. *Macromol. Chem. Phys.* **1994**, *195*, 1225. Samperi, F.; Puglisi, C.; Montaudo, G. *Macromol. Chem. Phys.* **1994**, *195*, 1240.
(23) Samperi, F.; Puglisi, C.; Montaudo, G. *J. Polym. Sci., Polym., Part A: Polym. Chem.* **1994**, *32*, 1807.
(24) Montaudo, G.; Puglisi, C.; de Leeuw, J. W.; Hartgers, W.; Kishore, K.; Ganesh, K. *Macromolecules* **1996**, *29*, 6466.
(25) Sturiale, L.; Montaudo, G.; Puglisi, C. *Macromolecules* **1999**, *32*, 2194−2200.
(26) Samperi, F.; Montaudo, M. S.; Montaudo, G.; Puglisi, C.; Sepulchre, M.; *Macromol. Chem. Phys.* **1996**, *197*, 2615−2625.
(27) Carroccio, S.; Puglisi, C.; Montaudo, G. *Macromol. Chem. Phys.* **1999**, *200*, 2345−2355.

MA0502349